The Visual Computer (2022) 38:419–432
https://doi.org/10.1007/s00371-020-02023-z

ORIGINAL ARTICLE

Visual complexity of shapes: a hierarchical perceptual learning model

Lingchen Dai[1] · Kang Zhang[2] · Xianjun Sam Zheng[3] · Ralph R. Martin[4] · Yina Li[5] · Jinhui Yu[1]

Accepted: 6 November 2020 / Published online: 6 January 2021

Abstract
Understanding how people perceive the visual complexity of shapes has important theoretical as well as practical implications. One school of thought, driven by information theory, focuses on studying the local features that contribute to the perception of visual complexity. Another school, in contrast, emphasizes the impact of global characteristics of shapes on perceived complexity. Inspired by recent discoveries in neuroscience, our model considers both local features of shapes: edge lengths and vertex angles, and global features: concaveness, and is in 92% agreement with human subjective ratings of shape complexity. The model is also consistent with the hierarchical perceptual learning theory, which explains how different layers of neurons in the visual system act together to yield a perception of visual shape complexity.

Keywords Neurons · Hierarchical · Shape · Visual complexity · Regression analysis

1 Introduction

When viewing objects constructed of different shapes, people perceive various levels of complexity. Differences in visual complexity have a bearing on information processing. For instance, it takes more time and cognitive effort to process complex shapes than simple ones [52]. Complex objects are easier to discriminate, but harder to remember. Simple objects, in contrast, are easier to remember, but harder to differentiate [29]. The level of complexity can also affect aesthetic perception. In general, objects or shapes with an intermediate degree of complexity receive the highest aesthetic ratings [22].

Understanding how people perceive the visual complexity of shapes has important theoretical as well as practical implications. On the one hand, it can advance knowledge of how our brains process information and aesthetics [14,48]. On the other hand, it can also provide guidance for interfaces for mobile phones, computer software, images, and web pages, and for the industrial design of such items as company logos, icons, and products of practical use [9,38,52]. Furthermore, understanding of human perception of shape complexity has important implications for the field of computer vision, for tasks such as shape analysis, pattern recognition, and object recognition [46,53].

What factors contribute to the perception of complexity? How can we predict perceived levels of shape complexity? Over the past 50 years, numerous studies have been conducted to explore this topic, and dozens of metrics have been proposed for computing shape complexity. However, despite all these efforts, there is a lack of systematic understanding or a cohesive model of how various parameters contribute to the perception of complexity.

One school of researchers, mostly influenced by information theory [44], suggests that shape complexity is directly associated with the amount of information contained in a shape. The more information or features a shape has, the more effort is required to process it; as a result, the shape is perceived as more complex. Mathematically, one can compute the entropy encoded by the shape to represent its degree of complexity [40]. The challenge, however, is which measures of entropy are most relevant to perceived complexity.

Attneave [2,3] was among the first group of researchers inspired by information theory to study visual complexity. A

✉ Jinhui Yu
jhyu@cad.zju.edu.cn

1 State Key Laboratory of CAD&CG, Zhejiang University, Hangzhou, Zhejiang, China

2 Department of Computer Science, University of Texas at Dallas, Dallas, TX, USA

3 Department of Psychology, Tsinghua University, Beijing, China

4 School of Computer Science and Informatics, Cardiff University, Cardiff, UK

5 School of Management, University of Science and Technology of China, Hefei, China

typical procedure used in these studies involved collecting human subjects' ratings of the visual complexity of a set of random polygons or shapes. Various metrics were then used to calculate the features of these shapes, which were correlated with the subjective ratings. A series of studies showed that the following metrics correlate with human perceptual ratings: the number of independent turns, angular variability [3], the perimeter of shape [42], the variance of interior angles, means of x and y coordinates, second moment of deviation of side length, variance of side lengths, largest radial length, perimeter length [8], and quantities derived from the contour, especially its concave parts [20].

One major drawback of these studies is that they were exploratory and the list of such metrics is endless. Researchers would often attempt to calculate as many metrics as they could think of, and report those that they found to be correlated with subjective ratings, without giving systematic psychological explanations. Indeed, Brown and Owen [8] found only a small subset of the proposed 80 or so measures being perceptually relevant.

In contrast to this bottom-up, local feature-driven approach , another school of researchers argues that the goal of human perception is to see higher order of structure, in other words, to extract higher-order invariants of visual information, such as affordances [49]. Therefore, they suggest that overall patterns or global characteristics of objects significantly impact people's perception of visual complexity.

This school of theory can be traced back to gestalt psychology [31], which argues that our perception tries to see the overall form, and to extract invariance. Attention is focused on the overall patterns of stimulation rather than small details [23]. For example, previous research has shown that symmetrical objects are perceived less complex [21]. van der Helm and Leeuwenberg [12] developed a holographic coding language to predict visual complexity of shapes, and the structural information in their code represents those shape regularities that are invariant under scaling. These results are also consistent with design principle that advocates symmetry, balance, and equilibrium, due to their increased order [5], and hence a reduced level of complexity.

In summary, researchers have proposed different metrics to measure the amount of information or local features contained in shapes, such as edge lengths and angles, as well as global shape characteristics, such as symmetry and balance. Though these findings contribute to the understanding of complexity, a unified understanding of the relationships of these metrics is necessary.

Recent advances in neuroscience, especially concerning how the human visual cortex encodes shape information, offer a possible reconciliation for the two schools of thought on visual complexity. The neuroscience findings shed light on several key characteristics of how our brains process visual information.

Such research has shown that visual information processing is hierarchical [13]. Hubel and Wiesel [27] first discover that different types of neurons exist in the visual cortex. Simple cells with a narrow receptive field only respond to lines having a particular orientation, and are often referred to as *line detectors*. Complex cells with bigger receptive fields respond best to moving edges in a specific direction, and are called *motion detectors*. Hypercomplex cells with large receptive fields respond best to edge changes, and are *angle detectors*. These three different types of neuron work together to decompose a visual shape into different parts for object recognition.

Since the pioneering work of Hubel and Wiesel, further research has shown that the perception of visual objects or shapes takes place in the ventral cortical pathway, i.e., the *what* pathway. First, the information is processed in the primary visual cortex (V1), and then the secondary cortex (V2). During these stages, shape information is encoded as local features, such as specific orientations in V1 [27], and combinations of orientations in V2. Studies have shown that in the intermediate stages (V3/V4), neurons encode shapes of intermediate complexity, and are sensitive to curvature [53]. At later stages, including the inferotemporal (IT) cortex and the lateral occipital complex (LOC), neurons encode more complex and global shape information, even including faces and places [28].

Information processing in the visual cortex is performed in a feedforward manner: information is propagated from the lower layers of the cortex to higher levels [35]. There is also a feedback loop from the higher levels to the lower ones. For instance, Murray et al. [39] use functional MRI to measure activity in LOC, a higher visual area for object shape perception, and in V1. They observed significantly increased activity in LOC and decreased activity in V1 when visual elements form coherent shapes. This supports the notion that the activity of neurons in lower levels is reduced when neurons in the higher levels can make sense of a visual stimulus.

Based on these neuroscience research findings, we hypothesize that both local and global features contribute to the perception of visual complexity, and that computational metrics which are biologically driven could better predict people's subjective ratings of visual complexity. For instance, at a higher level of the visual system, neurons are sensitive to coherent shapes and overall patterns [53]. This can be mapped to the global features of objects, such as unroundness or shape concaveness, consistent with Gestalt psychology's notion of seeking good forms. At lower levels of the visual cortex, neurons are specific and directly respond to the strength of the stimulus. For example, the edge length of a shape might be associated with the number of activated neurons. As the length of line increases, however, the activation may not scale linearly, but logarithmically. In addition, lower levels of neurons are sensitive to orientation change,

so vertex angle entropy might be a good measure of this stimulus.

Apart from 2D shape complexity, several researchers attempt to measure 3D shape complexity. In 2005, Rossignac [45] discussed several complexity measurements for 3D shapes, including algebraic complexity which measures the degree of polynomials needed to represent the shape exactly in its implicit or parametric form, topological complexity which measures the number of handles and components or the existence of non-manifold singularities, non-regularized components, holes or self-intersections, morphological complexity which measures the smoothness and feature size, combinatorial complexity which measures the vertex count in polygonal meshes, and representational complexity which measures the footprint and ease-of-use of a data structure, or the storage size of a compressed model. Butt and Biswas [17] used the orthogonal convex hull and an orthogonal convex skull are used together to derive the complexity of an object. Cortical-shape measure was proposed to represent localized shape complexity as the difference between the observed distribution of local surface topology [30]. Kwon et al. [33] introduced the concept of feature shape complexity and adopted it as the criterion for the simplification of feature-based 3D CAD models. Wimmer et al. [34] proposed total absolute curvature to quantify complexity of curved surface shapes aiming at style design.

3D objects exhibit different shapes from different views, a 3D object may appear quite simple from one view, and much more complex from another view. Also, the concepts of metrics for 3D shape complexity differ significantly from those for 2D shape complexity. We thus confine our study to 2D shape complexity and present our framework of shape complexity in the next section.

2 Overview of our approach

We use a regression model to describe polygon shape complexity, because regression analysis offers a rich set of tools for assessing both the proposed model and the significance of variables in the model. A regression model relates responses to predictor (or explanatory) variables via

$$C_i = X_i\beta + \varepsilon_i, \tag{1}$$

where C_i denotes the response for the ith sample observation ($i = 1, \ldots n$, where n is the number of observations), X_i is a set of predictor variables, and β denotes their weights. Noise is represented by error terms ε_i, assumed to have mean zero.

Having chosen a set of predictor variables, a model may be constructed by choosing β to minimize the sum of squared errors between the predictions $X_i\beta$ and the observations C_i. The optimal value of β is given by

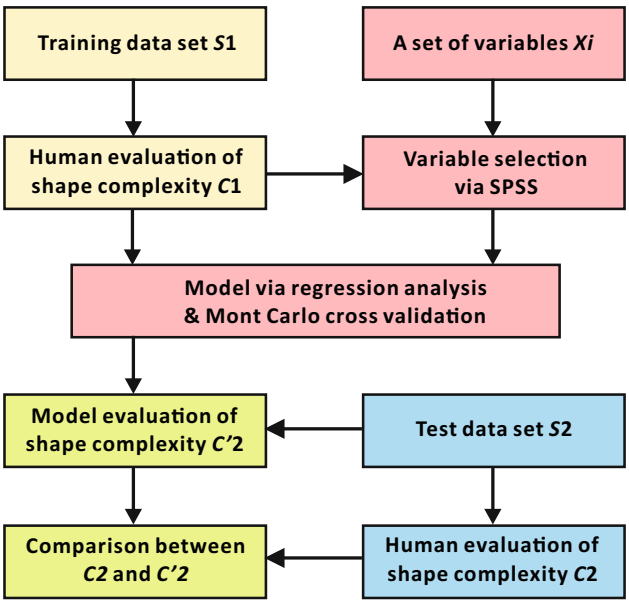

Fig. 1 Framework for developing models of shape complexity

$$\hat{\beta} = \arg\min_{\beta} \sum_{i=1}^{n} (C_i - X_i\beta)^2. \tag{2}$$

Figure 1 shows the framework of our approach. It starts from construction of a training data set S_1 and human evaluation of shape complexities as C_1 (yellow boxes). We then choose a set of variables X_i intended to capture certain features of a class of shapes reflecting their complexity, including both new variables and existing variables from previous works, as candidate predictors. We run variable selection via SPSS to automatically remove insignificant predictors of complexity, and obtain a linear regressor with fewer variables. To avoid over-fitting to the training data used in this process, we adopt Monte Carlo cross-validation to obtain the final regression model (pink boxes). We also evaluate our model using a separate test data set S_2, by comparing the model's prediction of complexity C_2' with the human evaluations C_2 on S_2 (blue and green boxes).

3 Construction of variables

3.1 Variables capturing local shape features

As stated earlier, a school of researchers, including Attneave [2], consider perception as a matter of processing information contained in shapes. In particular, they reason that the more information a shape has, the more effort is required to process it, so the shape would be perceived more complex. Shannon's information theory may be used to quantify the amount of information contained in a shape. Shannon entropy measures

the uncertainty associated with a random variable, i.e., the expected value of the information in a message.

Let X be a discrete random variable taking values x with distribution

$$p(x) = \Pr[X = x], \tag{3}$$

where $\Pr[X = x]$ is the probability of variable X taking value x. The entropy $H(X)$ of X is defined as

$$H(X) = -\sum_{x \in X} p(x) \log p(x). \tag{4}$$

and measures the average uncertainty of the random variable X. It quantifies the expected amount of information in the statement that X has a certain value, measured in bits with logarithms of base 2.

Next, we consider how to apply Eq. 4 to measure the entropy of vertex angles to obtain a local variable measuring shape complexity.

3.1.1 Weighted vertex angle entropy H'_α

Attneave [2] finds through experiment that information is concentrated along contours of shapes, particularly at those points of the contour where its direction changes most rapidly. Following Feldman and Singh [20], we consider a shape contour of length L, sampled at n uniformly spaced points separated by intervals $\Delta s = L/n$ (see Fig. 2). From point to point along the sampled curve, the tangent direction changes by an angle $\Delta\phi$, or α, called the *turning angle*. Feldman and Singh take α as a random variable and assume that α follows a von Mises distribution centered on $\alpha = 0$ [20]:

$$p(\alpha) = A \exp(b \cos(\alpha)), \tag{5}$$

where b is a parameter modulating the distribution and A is a normalizing constant (depending on b but not α). Positive values of α correspond to clockwise turns and negative values to counterclockwise turns. The von Mises distribution is the natural analog of a Gaussian (normal distribution) for angular measurements [26]. It agrees with a variety of empirical data, including the turning curves of orientation selective neurons in the primary visual cortex [50] as well as human observers' visual expectations about how smooth curves are likely to continue [19].

The angular entropy associated with α is then:

$$H(\alpha) = -p(\alpha) \log p(\alpha). \tag{6}$$

Combining Eqs. 4 and 5, one can calculate the angular entropy of a polygon, H_α, by treating each angle in the polygon independently, as done in Page et al. [40] and Feldman and Singh [20]. This gives a total angular entropy:

$$H_\alpha = \sum_{v \in P} H(\alpha(v)). \tag{7}$$

where v is the vertex of polygon P.

Unfortunately, the above approach overestimates the entropy in the presence of repeated angles, which are no longer independent. As noted by Attneave [2] in considering an ornamented ink bottle on the corner of a desk shown in Fig. 3, the 13 right angles on the left shoulder of the bottle contain less than 13 times the information of the angle in isolation at the corner of the table. Attneave attributes such information reduction to the repetitiveness of the pattern, without offering a quantitative measurement. We can use Eq. 4 to calculate the information associated with the repetitive pattern if its probability can be estimated.

If a turning angle α is repeated m times in a polygon, we may assume that α appears independently each time (as we do not know what is coming next), so the probability $p_m(\alpha)$ is:

$$p_m(\alpha) = \prod_{t=1}^{m} p(\alpha), \tag{8}$$

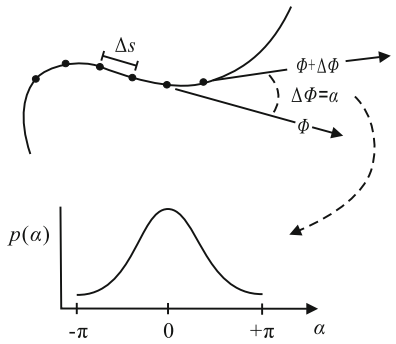

Fig. 2 Von Mises distribution of turning angles for a polygon

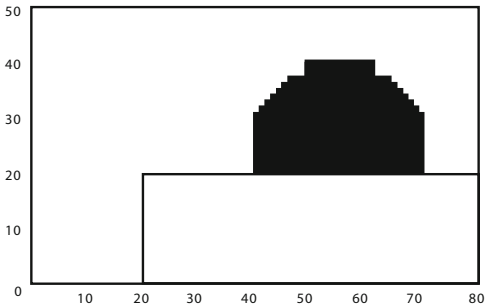

Fig. 3 Repetitive visual stimulation, following Attneave [2]

where $p(\alpha)$ is the probability of α appearing once. The corresponding entropy $H_m(\alpha)$ is:

$$H_m(\alpha) = -\prod_{t=1}^{m} p(\alpha) \log \prod_{t=1}^{m} p(\alpha). \tag{9}$$

It is easy to prove that

$$-\prod_{t=1}^{m} p(\alpha) \log \prod_{t=1}^{m} p(\alpha) < -\sum_{t=1}^{m} p(\alpha) \log\ p(\alpha). \tag{10}$$

Thus, the information contained in a repetitive pattern is smaller than the total information contained independently by the elements in the pattern. If several repetitive patterns appear in the polygon, we calculate their entropies using Eq. 9. The total entropy in a polygon is then the sum of entropies associated with non-repetitive patterns and entropies associated with repetitive patterns.

It is also apparent that in Fig. 3, vertices associated with longer edges (e.g., at the corner of the table) appear visually stronger than those adjacent to short edges (e.g., at the shoulder of the ink bottle). Based on this observation, we propose weighting angular entropy to take edge lengths into account:

$$H'_\alpha = \sum_{v \in P} w(v) H(\alpha(v)). \tag{11}$$

where $w(v)$ is the ratio of the area of the triangle defined by the vertex v and its two neighboring edges to the area of the entire polygon, and $\alpha(v)$ is the angle at v. Obviously, the maximum possible value of $w(v)$ is 1.

3.1.2 Weighted edge length information H'_L

Attneave [3] proposes that increasing the length of a line adds information, but at a decreasing rate. Using this psychological finding, we propose an empirical formula for directly estimating the information of the edge length as below:

$$H(l) = \log(1 + l). \tag{12}$$

where $l \geq 0$ is edge length. Obviously, $H(l)$ increases as l increases, but at a decreasing rate, which agrees with the experimental psychological findings.

As mentioned before, repetitive pattens may cause visual information redundancy [2]. Similar to the weight vertex angle entropy, given a segment of length l repeated n times, we define the information associated with this segment as

$$H(l) = \log(1 + l) * (1 + \ln(n)). \tag{13}$$

The total information of edge lengths H_L in a polygon can be obtained by summing the information for all the edges in the polygon:

$$H_L = \sum_{e \in p} H(l(e)). \tag{14}$$

where e is the edge of polygon P, and $l(e)$ is the length at e. Furthermore, polygons with greater variation in edge length appear more complex than those with less variation and, inspired by angular variability [3] that measures the average difference between adjacent angles in a polygon, we use the standard deviation of edge lengths in a polygon to weight the total information in the following fashion:

$$H'_L = (1 + D(l)) \sum_{e \in p} H(l(e)). \tag{15}$$

where $D(l)$ is the standard deviation of edge lengths.

3.2 Variables capturing global shape features

3.2.1 Concaveness C_V

Considering the global aspects of a shape contributing to its complexity, we start from concaveness. Concaveness may be measured by the difference in area between a polygon and its convex hull [7], and quantified as a ratio between 0 and 1:

$$C_V = (A_C - A)/A_C. \tag{16}$$

where A_C is the area of the convex hull, and A is the area of the polygon.

Both Brinkhoff et al. [7] and Su and Bouridane [49] have used Eq. 16 as an indicator of shape complexity, regarding a shape which strongly differs from its convex hull as complex. Our regression analysis (provided later) finds that this variable is not a significant predictor of complexity. We therefore seek a new measurement of convexity instead.

3.2.2 Convexity N'

The three shapes shown in Fig. 4 are taken from Psarra and Grajewski [42]. Although having an area much smaller than its convex hull, shape (c) visually appears simpler than shape (b). This is because four longer edges in shape (c) are drawn close enough for them to form an L shape which looks simple. The overall shape of (a) is close to a its convex hull, and thus looks also simpler than shape (b).

Figure 4 also shows that shape (c) differs more from its convex hull than shape (b) does. Let us consider a new variable N for measuring the convexity of a shape. It is inefficient and cumbersome to compute the shape's medial transform and use the radius associated with medial transform points to determine convexity. Instead, we first convert the polygon

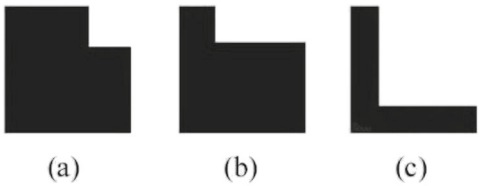

Fig. 4 Three L shapes, following Psarra and Grajewski [42]

under consideration into a binary image and then calculate a distance map for the polygon. The distance map labels each pixel inside the polygon with its distance to the nearest pixel on the boundary of the polygon. Let the maximal distance of the pixels in the distance map of the polygon be D_P. Let the maximal distance of the pixels in the distance map of the convex hull of the polygon be D_C. We use their ratio to measure the convexity of a given polygon shape:

$$N = D_P / D_C, \tag{17}$$

Clearly, N lies in the range [0,1]. N approaches 0 as the polygon approaches a thin curved line, indicating that the shape looks very concave globally. On the other hand, when N approaches 1, the polygon is close to its convex hull. One cannot, however, use N directly. As noted earlier, shape (b) appears most complex, while shape (c) has the minimum value of N among the three. Incorporating this characteristic, we perform a nonlinear transformation on N to obtain a new variable N':

$$N' = \sin(\pi N). \tag{18}$$

We have also experimented with other nonlinear transformations, such as $N'' = \sin(\pi N^2)$, and found the above notion to be the most appropriate.

3.2.3 Unroundness *M′*

We propose another global variable, unroundness M, and define it as the difference in area between the polygon A and its equivalent circle A_E (i.e., a circle whose perimeter equals that of the polygon):

$$M = (A_E - A)/A_E, \tag{19}$$

We again need to apply a nonlinear transformation to M for exactly the same reason as for N, and define a modified M:

$$M' = \sin(\pi M). \tag{20}$$

3.3 Other variables in existing models

In order to build the most effective model, we combine our variables described above with a range of variables taken from existing models [3,10,40]. These include.

Three variables from Attneave [3]: the number of turns C_T (i.e., changes in direction or corners), symmetry S (a symmetric object has a value 1 and an asymmetric one a value 0), and angular variability A_V (the average difference between adjacent angles in a polygon). Curvature entropy H_θ by Page et al. [40] is approximated by the turning angle. Three variables from Chen and Sundaram [10]: $V_1 = (1 + R)\min(C_{\text{dis}}, C_{\text{angle}})$, $V_2 = (1 + R)\max(C_{\text{dis}}, C_{\text{angle}})$, and $V_3 = (1 + R)P$, where C_{dis} is global distance, C_{angle} is local angle, P is a perceptual factor and R a randomness measure (for full definitions see Chen and Sundaram [10]). We also include C_{dis}, C_{angle} and P, R, totaling eleven existing variables.

These eleven variables, together with the previous five quantifies: edge length information H'_L, turning angle entropy H'_α, concaveness C_V, convexity N', and unroundness M', are taken as predictor variables X_i in our initial regressor. Table 1 summarizes all the sixteen representative variables measuring shape complexity.

We expect that any reasonable measure of shape complexity should be scale invariant, because our formula includes terms such as edge length information which is scale dependent. To ensure scale invariance, we normalize each shape in the training data set and the new data set mentioned later by dividing all distances in the shape by the mean distance between all pairs of vertices of the shape, following [4].

To determine the relative importance of each variable, we next normalize all the variables by feature scaling

$$x'_i = \frac{x_i - x_{\min}}{x_{\max} - x_{\min}}. \tag{21}$$

where x_i is the value of variable X_i, and $x_{\min}$ and $x_{\max}$ are its extremal values over all training and test shapes. We also use the same normalization method to calculate the average human evaluation score.

4 Human subjective ratings

Thirty shapes with different levels of complexity were selected from previous studies [2,5,36,42] as the training data set (shown in Fig. 5).

Thirty students (including undergraduates and postgraduates) were recruited, 17 male and 13 female, aged 18–31, from Zhejiang University, China, as subjects in the study. Each subject was individually presented with the user interface shown in Fig. 6. The experiment starts by presenting

Table 1 Sixteen measurements of visual complexity, including ours and representative ones from the literature

No.	Feature	Local versus global	Explanation	Formula	Biological relevance
1	Weighted edge length information	Local	The information of each edge in the polygon	$H'_L = (1 + D(l)) \log(l)$	High
2	Weighted vertex angle entropy	Local	The entropy of each vertex angle in the polygon	$H'_\alpha = \sum_{v \in P} w(v) \left[\sum_{v \in P} - p(\alpha) \log p(\alpha)\right]$	High
3	Number of turns	Local	The total number of independent sides or contour turns in the polygon	$C_T = \log(N)$	Medium
4	Angular variability	Local	The average difference between adjacent angles in the polygon	$A_V = \left(\sum_{v \in P} v_\alpha\right) / N$	Low
5	Curvature entropy	Global	The distribution of the vertex angles in the polygon	$H_\theta = -\sum_{\theta \in v} p(\theta) \log p(\theta)$	High
6	Concaveness	Global	The convex and concave character of the polygon	$C_V = (A_C - A)/A_C$	Medium
7	Convexity	Global	How much a polygonal differs from its convex hull	$N' = \sin[\pi(D_P/D_C)]$	High
8	Unroundness	Global	How much a shape differs from its equivalent circle	$M' = \sin[\pi(A_E - A)/A_E]$	High
9	Symmetry	Global	The symmetry of the polygon	$S = \begin{cases} 1 \; symmetry \\ 0 \; not \end{cases}$	Medium
10	Perceptual Smoothness	Global	Local angles with large value appear smoother.	$P = \frac{1}{N} \sum \left(e^{(-\theta_i/\pi)} - e^{-1}\right) / \left(1 - e^{-1}\right)$	Medium
11	Local angle	Local	The local angle information of a polygonal shape	$C_{\text{angle}} = \min\left(\frac{H_{J,angle}}{\log_2 N} + \frac{e_{J,angle}}{e_{max}}\right)$	Low
12	Global distance	Global	The entropy of the distance between each contour point and the center	$C_{\text{dis}} = \min\left(\frac{H_{J,dis}}{\log_2 N} + \frac{e_{J,dis}}{e_{max}}\right)$	Medium
13	Randomness	Global	The distance between two traces starting from two points with maximum distance	$R = d(A_{S_1}, A_{S_2})$	Low
14	V_1	Global	Simpler descriptors are more important in shape simplicity	$V_1 = (1 + R) \min(C_{\text{dis}}, C_{\text{angle}})$	Low
15	V_2	Local	More complex descriptors are less important in shape simplicity.	$V_2 = (1 + R) \max(C_{\text{dis}}, C_{\text{angle}})$	Low
16	V_3	Global	See the 10th and 13th rows	$V_3 = (1 + R) P$	Low

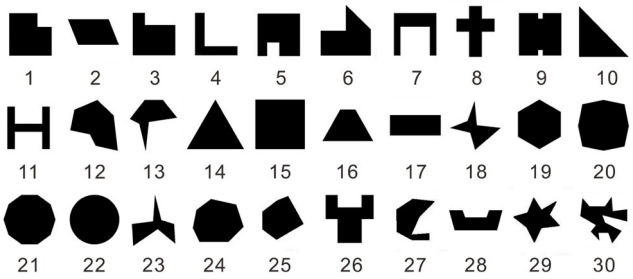

Fig. 5 The training data set with different levels of complexity selected for this study

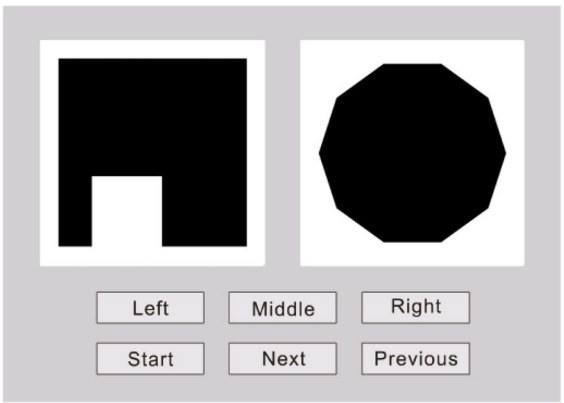

Fig. 6 The user interface for pairwise comparison

two different shapes randomly selected from the experimental data set. The subjects indicated which shape they perceive to be more complex by clicking the *Left* or *Right* button. They can also click the *Middle* button to indicate no perceived difference in complexity between the two shapes. A score of 1 is given to the more complex shape and 0 to the other shape, or 0.5 to each if no difference. The subject then clicks the *Next* button to retrieve the next pair of shapes. The experiment terminates when all shape pairs have been scored. To reconsider the previous decision, a subject could push the *Previous* button to redisplay the previous pair of shapes and redo the comparison. With a total of 435 (30×29) pairwise comparisons, the study took each participant about 20 min to complete.

We sum the scores given to each shape and average the results for all the subjects. Divided by the number of shapes, complexity values are normalized within the range [0,1].

5 Regression analysis

Some predictors of shape complexity use a single variable [40,42,44], while others are based on multiple variables. Typically, a linear combination of multiple variables is used with weights assigned heuristically or experimentally [7,10, 49]. Determination of those weights remains generally unaddressed. Attneave used regression models [2] to analyze the relationships between manually judged complexity and various explanatory variables based on geometric properties of shapes. We also use regression analysis to obtain the final model. We determine which variables make little contribution to the model by running the variable selection procedure in SPSS to automatically remove variables that are not significant predictors of complexity, and obtain a linear regressor with three variables.

In linear regression analysis, the fitting process optimizes the model parameters to make the model fit the training data as well as possible. It generally turns out that the fitted relationship appears to perform poorer on a new data set than on the data set used for fitting [18]. This is called overfitting, likely to happen when the size of the training data set is small. An overfit model has poor predictive performance, as it overreacts to minor fluctuations in the training data. Using a larger training set would, however, reduce the effectiveness of the subjective scores, due to the quadratically increasing experimental time needed for pairwise comparisons, and thus subjects' lack of concentration. We therefore derive a more accurate estimate of model prediction using the Monte Carlo cross-validation [16].

5.1 Monte Carlo cross-validation

Monte Carlo cross-validation is a simple yet effective method to avoid an unnecessarily large model. It reduces the risk of overfitting of the data [54], and has been shown asymptotically consistent [47]. In Monte Carlo cross-validation, the data set (of size n) is randomly split into complementary subsets: a training set S_t (of size n_t) and a testing set S_v (of size n_v, $n_v = n - n_t$). We set n_v 33% of n, as suggested in [24], perform regression analysis on the training set, and then validate the analysis on the other subset. In this manner, multiple rounds of cross-validation are performed using different partitions, and the validation results are averaged over the rounds.

In this study, 10 rounds of Monte Carlo cross-validation are performed using different partitions, and the results are averaged over the rounds. Our equation of final regression model for perceived complexity is

$$C = 0.676H'_L + 0.262N' + 0.142H'_\alpha + 0.051 \quad (22)$$

Table 2 shows the statistics of our model. The model using three predictors is able to explain 91.6% of the variance in shape complexity, and statistically significant ($Sig. = 0.000$). Our model can therefore efficiently describe the perception of shape complexity. All predictors make significant contributions as their associated p values are lower than 0.05. The coefficients H'_L, N' and H'_α ($Reg.Coef$ column) indicate that H'_L plays more important role than the other two predic-

Table 2 Statistics of final regression model

Var.	$R^2 = 0.929$ Reg. Coef.	Adj. $R^2 = 0.916$ Std. Er.	Std. Er. = 0.072 Std. Coef.	$F = 72.224$ t	Sig. = 0.000 Sig.
H'_L	0.676	0.177	0.496	5.317	0.001
N'	0.262	0.063	0.439	4.735	0.002
H'_α	0.142	0.057	0.250	2.666	0.031
(Const.)	0.051	0.038		1.498	0.263

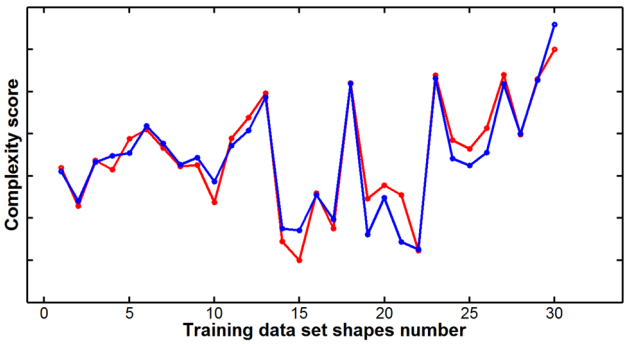

Fig. 7 Complexity scores of the training data set with 30 shapes evaluated by the subjects (in red) and the linear regressor (in blue)

Table 3 Statistics of performances associated with different models over 10 rounds

	S_t	S_v
Average $R_P/Sig.$	0.964/0.000	0.959/0.000
Average $R_S/Sig.$	0.943/0.000	0.918/0.000
Average $\tau/Sig.$	0.824/0.000	0.796/0.000
SD of $R_P/Sig.$	0.007/0.000	0.009/0.000
SD of $R_S/Sig.$	0.004/0.000	0.020/0.000
SD of $\tau/Sig.$	0.013/0.000	0.022/0.000
Average of MSE	0.004	0.009
SD of MSE	0.001	0.003

tors in predicting the human perceived complexity of shapes. Both regression analysis and deep learning are inspired by the human neural hierarchical structure. Although a deep learning approach is now widely used in image and pattern recognition [6,43], training a deep learning model needs a massive dataset. Our training dataset is not big enough for training a good deep learning model. On the other hand, our model can generate meaningful features (edge length, vertex angle entropy, convexity) that enable users to understand exactly how given shapes are measured, rather than simply output a result in a black-box fashion, such as [15,37].

To aid further understanding of the above statistics, Fig. 7 illustrates the complexity scores of the training data set with thirty shapes evaluated by the subjects (red line) and regressor (blue line) .

5.2 Bivariate correlation analysis

To evaluate the effectiveness of our regression model, we conduct bivariate correlation analysis. Previous research has performed various kinds of non-parametric bivariate correlation analysis, including Pearson correlation test, Spearman's rank correlation test and Kendall rank correlation test [25,41], to compare values of visual complexity assessed by humans and by computer models. These tests rank values to assess relationships. Kendall rank test is usually preferred to Spearman's rank correlation test for a small data set with a large number of tied ranks.

Table 3 shows three average correlation coefficients and associated 2-tailed Significance (Pearson correlation coefficient, denoted as Average $R_P/Sig.$; Spearman's rank correlation coefficient, denoted as Average $R_S/Sig.$; Kendall rank correlation coefficient, denoted as Average $\tau/Sig.$), for both the training sets (S_t) and the testing sets (S_v). They serve to evaluate the average prediction performances of our regression models on different training and testing sets. We also show the average mean squared error (denoted as Average MSE) [32] between model evaluated scores and manually evaluated scores over 10 rounds, the standard deviation (SD) of three average correlation coefficients and MSE over 10 rounds for both training and testing sets to evaluate the variation of prediction performances in Table 3. The table clearly shows that our regression models yield a highly significant correlation between human and computer evaluated results with high accuracy since the three average correlation coefficients are high and associated average $Sig.$ are less than 0.05 with low average MSE. Furthermore, the low SD of correlation coefficients and MSE indicate that the variation of prediction performances is small over 10 rounds. Our regression models provide prediction of high accuracy and the explanatory variables in regression models are of high predictive power in shape complexity evaluation.

Figure 8 shows the average R_P, R_S, τ and average MSE over regression models of shape complexity for 10 rounds, where red lines represent the training set and blue lines the testing set. The regression models indeed show high performances with high average R_P, R_S, τ and low average MSE for both training and testing sets.

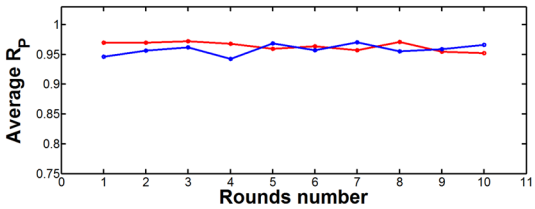

(a) Average R_P correlation coefficient

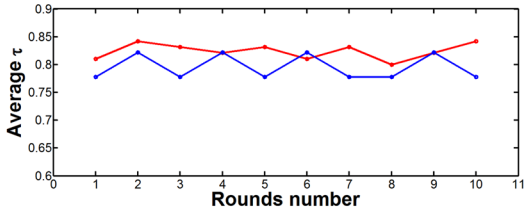

(b) Average τ correlation coefficient

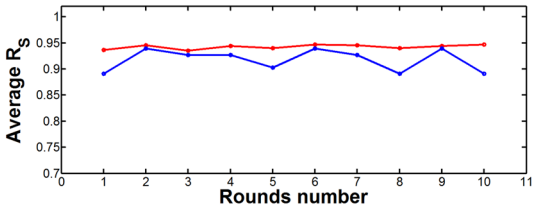

(c) Average R_S correlation coefficient

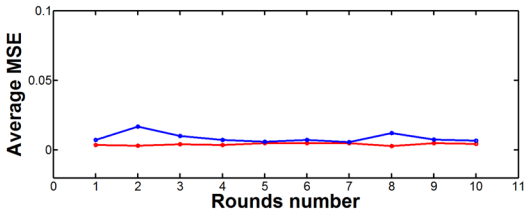

(d) Average MSE

Fig. 8 Performance curves with **a** average R_P correlation coefficient, **b** average τ correlation coefficient, **c** average R_S correlation coefficient and **d** average MSE over regression models for 10 rounds

6 Model test with a new data set

We further verify whether our regression model is effective for a new set of shapes. We use the new set of 30 shapes shown in Fig. 9, again selected from the previously used shapes [2, 5,14,42]. We also made modifications to several shapes by adding small notches along their boundaries, to make them more complex than the original ones. We conducted another user study to assess the complexity of the new set. The scores evaluated by the same group of subjects are shown by the red line in Fig. 10. We use the regression model (Table 2) to compute the complexity of each of those 30 shapes, with the results shown as the blue line in Fig. 10.

Table 4 shows the three correlation coefficients and associated 2-tailed Significance and mean squared error (MSE) between the model results and the manually evaluated scores for the new data set. Again, our regression model clearly yields a highly significant correlation between human and computer evaluated results with high accuracy, since the three average correlation coefficients are high and associated average $Sig.$ are less than 0.05 with low average MSE. This indicates that our regression model also has high prediction performances for the new data set.

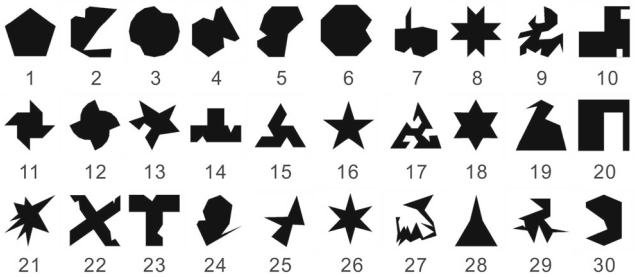

Fig. 9 The new set of shapes

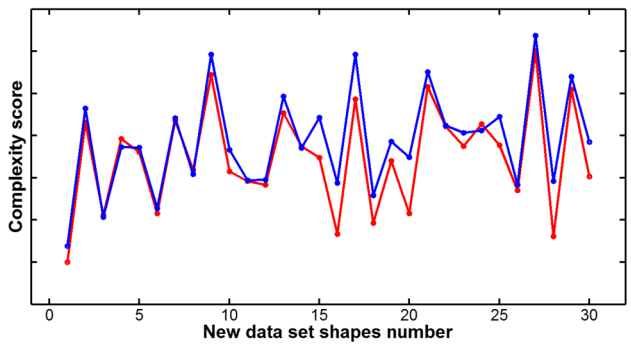

Fig. 10 Complexity scores of the new set of 30 shapes evaluated by subjects (in red) and the regression model (in blue)

Table 4 Correlation coefficients and MSE between the model results and the human evaluated scores for the new set

$R_P/Sig.$	0.937/0.000
$R_S/Sig.$	0.939/0.000
$\tau/Sig.$	0.798/0.000
MSE	0.014

7 Comparison to other methods

Table 5 compares our method with other 3 methods, i.e., Chen's model [10], Attneve's model [3] and Page's model [40], by Pearson correlation test (R_P), Spearman's rank correlation test (R_S), Kendall rank correlation test (τ), and mean squared error (MSE). It also shows that Page's model performs better than Chen's model and Attneave's model, but poorer than our method (see the statistics in Table 4).

Table 5 Correlation coefficients and MSE between results of other 3 models and the human evaluated scores for the new data set

	Chen	Attneave	Page
$R_P/Sig.$	0.633/0.000	0.623/0.000	0.818/0.000
$R_S/Sig.$	0.642/0.000	0.496/0.005	0.840/0.000
$\tau/Sig.$	0.490/0.000	0.382/0.003	0.668/0.000
MSE	0.043	0.047	0.037

8 Discussions

8.1 Both global and local features contribute to visual complexity

Our results clearly show that both global and local features contribute to the perception of visual complexity of shapes, thus agree with biological studies [27,28]. Specifically, the final linear regression model includes one global feature, i.e., concaveness, and two local features, i.e., edge length entropy and turning angle entropy. The three variables combined can account for approximately 92% variance of human subjective rating of the complexity of the same shapes. The performance is superior to earlier results [2,10,40]. This supports our initial hypothesis that both global and local features of shapes are important during information processing in determining visual complexity. Therefore, both schools of researchers, i.e., on information theory, such as Attneave [2], and on global invariance [11], are partially correct.

8.2 Biologically relevant statistical features correlated better with human subjective ratings

One may ask why the three features play a more important role in human perception of shape complexity than the other 13 selected features. We argue that these three features are more biologically relevant. For instance, edge length is directly associated with *line detectors* of simple cells, and turning angle is also associated with *angle detectors* of hypercomplex cells, in both V1 and V2 areas [27]. Unlike V2, V4 is tuned for object features of intermediate complexity, like simple geometric shapes. Therefore, global features, such as unroundness and concaveness, are more related to the V4 area or even higher areas, such as IT and LOC [53]. The other features, such as number of turns, angular variability, symmetry, or randomness, are less biologically relevant. Even though partially account for the variance of human perception, they are not significant enough to be included in the final regression model. These results are also consistent with Zheng et al.'s [55] findings that biologically relevant statistical features correlate better with human subjective ratings of web page complexity.

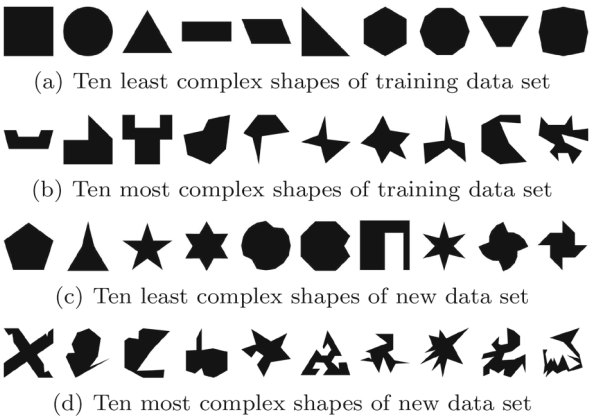

Fig. 11 Ten least/most complex shapes among the two sets as determined by our model

8.3 Hierarchical perceptual model of visual complexity

How do local and global features interact with each other to yield the perception of shape complexity? We believe that the hierarchical perceptual model proposed by Ahissar offers feasible explanations [1]. Ahissar categorizes neurons into three hierarchical levels: the lower, intermediate, and higher levels; neurons at the lower levels are more peripheral and specific for information coding and higher levels are more central and generic. She proposes that the visual processing of stimuli takes place first not at the lowest nor at the highest levels, but at intermediate levels, where neurons are selective for generic perceptual objects. If the processing is successfully accomplished, then neurons at the lower levels are not activated. The principle is that lower-level neurons are recruited for a visual perceptual task only when needed. Additional analysis by lower peripheral visual neurons takes time and resources, as demonstrated by feature combination processing [51].

According to Ahissar's hierarchical perceptual learning model [1], when viewing a common and simple shape, such as a *circle*, intermediate levels of neurons are activated and converge at higher levels, producing perception and behavior appropriate to the concept of the *circle*, e.g., a ball, while lower and peripheral neurons are not involved in this processing. Most complex and less common shapes, however, cannot be analyzed by higher levels in the perceptual hierarchy alone. Peripheral and specific neurons are recruited to process the information, resulting in simultaneous activations of neurons at multiple levels of the hierarchy.

Figure 11a, c shows the top ten least complex shapes among the two data sets as determined by our model. These shapes have strong global features, such as concaveness, and weak local features. In contract, shapes with weak global features and strong local features, e.g., Fig. 11b, d, are con-

sidered complex and less common. This is consistent with the hierarchical perceptual learning model that the activity of neurons at a lower-level decreases when neurons at a higher level can *explain* a visual stimulus.

9 Conclusions

Inspired by the latest empirical neuroscience evidence and perceptual learning theory, we have proposed a multi-level model of visual complexity, taking into account both local and global features. Our final regression model based on only three predictors can explain 92% of the variance in shape complexities determined by human subjects. Monte Carlo cross-validation allows us to sacrifice fitting accuracy to the training data to provide better generalization to new data. Our major contributions are twofold. First, our computational metrics are biologically inspired, and therefore can better predict subjective perception of visual complexity. Second, we have proposed a model based on the reversed hierarchical theory which integrates various complexity metrics.

Future study needs to validate our model with more data sets, and also to provide better understanding of the relationships between various parameters. We also wish to extend this work to practical applications, e.g., the complexity of logos, application program icons. Since more visual information, such as color, is involved in practical application, we plan to design new user studies capable of effectively evaluating the complexities of shapes and colors, and to explore new predictive variables suitable for color perception.

References

1. Ahissar, M.: Perceptual learning. Curr. Dir. Psychol. Sci. **8**, 124–128 (1999)
2. Attneave, F.: Some informational aspects of visual perception. Psychol. Rev. **61**(3), 183–193 (1954)
3. Attneave, F.: Physical determinants of the judged complexity of shapes. J. Exp. Psychol. **53**(4), 221–227 (1957)
4. Belongie, S., Malik, J., Puzicha, J.: Shape matching and object recognition using shape contexts. IEEE Trans. Pattern Anal. Mach. Intell. **24**(4), 509–522 (2002)
5. Birkhoff, G.D.: Aesthetic Measure. Harvard University Press, Cambridge (1933)
6. Brehar, R., Mitrea, D.A., Vancea, F., Marita, T., Nedevschi, S., Lupsor-Platon, M., Rotaru, M., Badea, R.I.: Comparison of deep-learning and conventional machine-learning methods for the automatic recognition of the hepatocellular carcinoma areas from ultrasound images. Sensors **20**(11), 3085 (2020)
7. Brinkhoff, T., Kriegel, H.P., Schneider, R., Braun, A.: Measuring the complexity of polygonal objects. In: Proceedings of 3rd ACM International Workshop on Advances in Geographical Information Systems, pp. 109–117. Citeseer (1995)
8. Brown, D.R., Owen, D.H.: The metrics of visual form: methodological dyspepsia. Psychol. Bull. **68**(4), 243–259 (1967)
9. Carballal, A., Fernandez-Lozano, C., Rodriguez-Fernandez, N., Santos, I., Romero, J.: Comparison of outlier-tolerant models for measuring visual complexity. Entropy **22**(4), 488 (2020)
10. Chen, Y., Sundaram, H.: Estimating complexity of 2D shapes. In: Proceedings of 7th Workshop on Multimedia Signal Processing, pp. 1–4 (2005)
11. Der Helm, P.A.V.: Simplicity versus likelihood in visual perception: from surprisals to precisals. Psychol. Bull. **126**(5), 770–800 (2000)
12. Der Helm, P.A.V., Leeuwenberg, E.: Goodness of visual regularities: a nontransformational approach. Psychol. Rev. **103**(3), 429–456 (1996)
13. Diaconescu, A.O., Litvak, V., Mathys, C., Kasper, L., Friston, K.J., Stephan, K.E.: A computational hierarchy in human cortex. arXiv preprint arXiv:1709.02323 (2017)
14. Donderi, D.C.: Visual complexity: a review. Psychol. Bull. **132**(1), 73–97 (2006)
15. Dou, Q., Zheng, X.S., Sun, T., Heng, P.A.: Webthetics: quantifying webpage aesthetics with deep learning. Int. J. Hum. Comput Stud. **124**, 56–66 (2019)
16. Dubitzky, W., Granzow, M., Berrar, D.P.: Fundamentals of Data Mining in Genomics and Proteomics. Springer, New York (2007)
17. Dutt M.B.A.: Boundary and Shape Complexity of a Digital Object. Lecture Notes in Computer Science Book Series 10149, pp. 105–117 (2017)
18. Everitt, B., Skrondal, A.: The Cambridge Dictionary of Statistics, vol. 106. Cambridge University Press, Cambridge (2002)
19. Feldman, J.: Bayesian contour integration. Attent. Percept. Psychophys. **63**(7), 1171–1182 (2001)
20. Feldman, J., Singh, M.: Information along contours and object boundaries. Psychol. Rev. **112**(1), 243–252 (2005)
21. Gartus, A., Leder, H.: Predicting perceived visual complexity of abstract patterns using computational measures: the influence of mirror symmetry on complexity perception. PLoS ONE **12**(11), e0185276 (2017)
22. Gellmann, M., Lloyd, S.: Information measures, effective complexity, and total information. Complexity **2**(1), 44–52 (1996)
23. Graham, L.: Gestalt theory in interactive media design. J. Hum. Soc. Sci. **2**(1), 571 (2008)
24. Haddad, K., Rahman, A., Zaman, M.A., Shrestha, S.: Applicability of monte carlo cross validation technique for model development and validation using generalised least squares regression. J. Hydrol. **482**, 119–128 (2013)
25. Harper, S., Jay, C., Michailidou, E., Quan, H.: Analysing the visual complexity of web pages using document structure. Behav. Inf. Technol. **32**(5), 491–502 (2013)
26. Hawkins, D.M., Lombard, F.: Cusum control for data following the von mises distribution. J. Appl. Stat. **44**(8), 1319–1332 (2017)
27. Hubel, D.H., Wiesel, T.N.: Receptive fields and functional architecture of monkey striate cortex. J. Physiol. **195**(1), 215–243 (1968)
28. Kanwisher, N.: Functional specificity in the human brain: A window into the functional architecture of the mind. Proc. Nat. Acad. Sci. USA **107**, 11163–11170 (2010)
29. Kayaert, G., Wagemans, J.: Delayed shape matching benefits from simplicity and symmetry. Vis. Res. **49**(7), 708–717 (2009)
30. Kim, S., Lyu, I., Fonov, V., Vachet, C., Hazlett, H., Smith, R., Piven, J., Dager, S., Mckinstry, R., Pruett, J., Evans, A., Collins, D., Botteron, K., Schultz, R., Gerig, G., Styner, M.: Development of cortical shape in the human brain from 6 to 24 months of age via a novel measure of shape complexity. NeuroImage **35**, 163–176 (2016)
31. Koffka, K.: Principles of Gestalt Psychology, vol. 44. Routledge, Abingdon (2013)
32. Konovalov, D.A., Sim, N., Deconinck, E., Heyden, Y.V., Coomans, D.: Statistical confidence for variable selection in qsar models via

monte carlo cross-validation. J. Chem. Inf. Model. **48**(2), 370–383 (2008)
33. Kwon, S.: Mun DKBHS: feature shape complexity: a new criterion for the simplification of feature-based 3d cad models. Int. J. Adv. Manuf. Technol. **88**(5–8), 1–13 (2017)
34. Matsumoto, T., Sato, K., Matsuoka, Y., Kato, T.: Quantification of "complexity" in curved surface shape using total absolute curvature. Comput. Graph. **78**(10), 108–115 (2019)
35. Maunsell, J.H.R., Newsome, W.T.: Visual processing in monkey extrastriate cortex. Annu. Rev. Neurosci. **10**(1), 363–401 (1987)
36. Mavrides, C.M., Brown, D.R.: Discrimination and reproduction of patterns: feature measures and constraint redundancy as predictors. Attent. Percept. Psychophys. **6**(5), 276–280 (1969)
37. McCormack, J., Lomas, A.: Understanding aesthetic evaluation using deep learning. In: International Conference on Computational Intelligence in Music, Sound, Art and Design (Part of EvoStar), pp. 118–133. Springer (2020)
38. Mcdougall, S., De Bruijn, O., Curry, M.B.: Exploring the effects of icon characteristics on user performance: the role of icon concreteness, complexity and distinctiveness. J. Exp. Psychol. Appl. **6**(4), 291–306 (2000)
39. Murray, S.O., Kersten, D., Olshausen, B.A., Schrater, P., Woods, D.L.: Shape perception reduces activity in human primary visual cortex. Proc. Nat. Acad. Sci. USA **99**, 15164–15169 (2002)
40. Page, D.L., Koschan, A., Sukumar, S.R., Rouiabidi, B., Abidi, M.A.: Shape analysis algorithm based on information theory. In: Proceedings of International Conference on Image, vol. 1, pp. 229–232 (2003)
41. Perkio, J., Hyvarinen, A.: Modelling image complexity by independent component analysis, with application to content-based image retrieval. In: Proceedings of 19th International Conference Artificial Neural Networks, pp. 704–714 (2009)
42. Psarra, S., Grajewski, T.: Describing shape and shape complexity using local properties. In: Proceedings of 3rd International Space Syntax Symposium, pp. 28.1–28.16. Citeseer (2001)
43. Rashid, M., Khan, M.A., Alhaisoni, M., Wang, S.H., Naqvi, S.R., Rehman, A., Saba, T.: A sustainable deep learning framework for object recognition using multi-layers deep features fusion and selection. Sustainability **12**(12), 5037 (2020)
44. Rigau, J., Feixas, M., Sbert, M.: An information-theoretic framework for image complexity. In: Computational Aesthetics in Graphics, Visualization and Imaging, pp. 177–184 (2005)
45. Rossignac, J.: Shape complexity. Vis. Comput. **21**(12), 985–996 (2005)
46. Serre, T., Wolf, L., Poggio, T.: Object recognition with features inspired by visual cortex. Comput. Vis. Pattern Recognit. **2**, 994–1000 (2005)
47. Severeyn, E., Velásquez, J., Herrera, H., Perpiñan, G., Wong, S., Altuve, M.: Estimation of invasive physiological parameters from non invasive parameters using dimensionless numbers and Monte Carlo cross-validation. In: 2019 XXII Symposium on Image, Signal Processing and Artificial Vision (STSIVA), pp. 1–5. IEEE (2019)
48. Sieu, B., Gavrilova, M.: Biometric identification from human aesthetic preferences. Sensors **20**(4), 1133 (2020)
49. Su, H., Bouridane, A., Crookes, D.: Scale adaptive complexity measure of 2D shapes. In: Proceedings of 18th International Conference of Pattern Recognition, vol. 2, pp. 134–137 (2006)
50. Swindale, N.V.: Orientation tuning curves: empirical description and estimation of parameters. Biol. Cybern. **78**(1), 45–56 (1998)
51. Treisman, A.: Perceptual grouping and attention in visual search for features and for objects. J. Exp. Psychol. Hum. Percept. Perform. **8**(2), 194 (1982)
52. Tuch, A.N., Bargas-Avila, J.A., Opwis, K., Wilhelm, F.H.: Visual complexity of websites: effects on users' experience, physiology, performance, and memory. Int. J. Hum Comput Stud. **67**(9), 703–715 (2009)
53. Ullman, S., Vidalnaquet, M., Sali, E.: Visual features of intermediate complexity and their use in classification. Nat. Neurosci. **5**(7), 682–687 (2002)
54. Xu, Q., Liang, Y., Du, Y.: Monte carlo cross-validation for selecting a model and estimating the prediction error in multivariate calibration. J. Chemom. **18**(2), 112–120 (2004)
55. Zheng, X.S., Chakraborty, I., Lin, J.J., Rauschenberger, R.: Correlating low-level image statistics with users—rapid aesthetic and affective judgments of web pages. In: Proceedings of the SIGCHI Conference on Human Factors in Computing Systems, pp. 1–10 (2009)

Lingchen Dai is a Ph.D. student in the State Key Laboratory of CAD and CG, Zhejiang University, Hangzhou, China. His research interests include computer graphics and computer vision.

Kang Zhang is Professor and Director of Visual Computing Lab, Department of Computer Science at the University of Texas at Dallas. He received his B.Eng. in Computer Engineering from University of Electronic Science and Technology of China in 1982, Ph.D. from University of Brighton, UK, in 1990, and Executive MBA from the University of Texas at Dallas in 2011. Prior to joining UT-Dallas, he held academic positions in the UK, Australia, and China. Dr. Zhang's current research interests include visual languages, aesthetic computing, generative art, and software engineering and has published over 250 papers in these areas. He has authored and edited seven books.

Xianjun Sam Zheng is Research Director of Tsinghua Happiness Technology Lab (H+Lab) and also an adjunct professor of psychology at Tsinghua University, Beijing. His research interests include aesthetic perception and computing, user experience and AI, and human–machine relationships.

Ralph R. Martin received the Ph.D. degree from Cambridge University in 1983. He is currently a Professor with Cardiff University. He has authored over 250 papers and 14 books, covering such topics as solid and surface modeling, intelligent sketch input, geometric reasoning, reverse engineering, and various aspects of computer graphics. He is a Fellow of the Learned Society of Wales, the Institute of Mathematics and its Applications, and the British Computer Society. He is on the Editorial Boards of Computer Aided Design, Computer Aided Geometric Design, Geometric Models, International Journal of Shape Modeling, CAD and Applications, and International Journal of CAD-CAM. He received the Friendship Award, China's highest honor for foreigners.

Yina Li received the Ph.D. degree from Southeast University at Nanjin in 2013. Her research interests include consumer visual information processing.

Jinhui Yu received the BSc and MSc degrees in electronics engineering from Harbin Shipbuilding Engineering Institute, Harbin Engineering University, China, in 1982 and 1987, respectively. He received the Ph.D. degree in computer graphics from the University of Glasgow in 1999. He is a professor of computer science at the State Key Lab of CAD & CG, Zhejiang University, China. He is also a guest professor at the Department of Computer Science, Harbin Finance University, China. His research interests include image-based modeling, non-photorealistic rendering, computer animation, and computer graphics art.